Effect of Thiazole Derivatives on Copper Corrosion in Acidic Sulphate Solution

Jelena Nakomčić[1], Gyöngyi Vastag[1,*], Abdul Shaban[2], Lajos Nyikos[2]

[1]University of Novi Sad, Faculty of Sciences, Trg Dositeja Obradovića 3, 21000 Novi Sad, Serbia
[2]Research Centre for Natural Sciences, Hungarian Academy of Sciences, Magyar tudósok körútja 2, 1117 Budapest, Hungary
*E-mail: djendji.vastag@dh.uns.ac.rs

Inhibition of copper corrosion in 0.1 mol dm^{-3} Na$_2$SO$_4$ solution (pH 3) by two thiazole derivatives of 5-(5'-methylfurfurylidene-2')-2,4-dioxotetrahydro-1,3-thiazole (MFDT) and 2-thiono-5-(4'-ethoxybenzylidene)-4-oxotetrahydro-1,3-thiazole (TEBOT) was studied by weight loss and potentiostatic polarization measurements. Inhibition efficiency follows the order: TEBOT > MFDT. The adsorption of each inhibitor on copper surface obeys Bockris-Swinkels adsorption isotherm ($X = 1$). Kinetic and thermodynamic parameters of corrosion processes were calculated and discussed.

1. INTRODUCTION

Copper is one of the most important nonferrous materials [1], having favorable properties such as mechanical workability, electrical and thermal conductivity [2,3]. It is widely used in construction, chemical, electrical and electronic industries [4]. Although copper is resistant to the influence of atmosphere and many chemicals, it is known that it is susceptible to corrosion in aggressive environments. Among so many methods in the corrosion protection, the application of corrosion inhibitors is one of the most important [5]. The protection using inhibitors involves modification of the metal surface via adsorption of inhibitor molecules which form a protective layer [6]. Most of the corrosion inhibitors are heterocyclic organic compounds containing N, S or O atoms [7,8]. Molecules that, at the same time, contain N and S in their structures show excellent inhibition performance in comparison with those containing only N or S [9,10]. So far, different types of compounds have been investigated to act as copper inhibitors. Antonijevic and Petrovic [11] fully studied the copper corrosion inhibitors in order to find models that can enable prediction of possibilities of newly

synthesized compounds to act as corrosion inhibitors and serve as guidance for future research, combining theory and practical investigations of substances with similar structure.

As an important kind of organic compound, thiazole derivatives whose molecules containing aromatic ring with both N and S atoms have desirable characteristics in inhibiting action. Apart from that, they exhibit several biological activities like antitumor and cytotoxic, anti-inflammatory, antimicrobial, antioxidant, antifungal, antitubercular, anticonvulsant and neuroprotective, diuretic, etc. [12]. Thiazole derivatives were investigated as inhibitors for corrosion of metals in the acidic or neutral media, such as zinc in HCl [13], aluminium alloy 2024 in neutral chloride solution [14], mild steel in formic, acetic acid solutions [15], and H_2SO_4 [16], copper in acidic Na_2SO_4 solution [17]. Obtained results showed that the thiazole-type compounds could be considered as effective potential inhibitors. However, a perusal of literature revealed that the use of them as inhibitors for copper corrosion in acidic media has been rarely reported.

The purpose of this paper is to evaluate two thiazole derivatives, namely 5-(5'-methylfurfurylidene-2')-2,4-dioxotetrahydro-1,3-thiazole (MFDT) and 2-thiono-5-(4'-ethoxybenzylidene)-4-oxotetrahydro-1,3-thiazole (TEBOT), as corrosion inhibitors for copper in 0.1 mol dm^{-3} Na_2SO_4 solution (pH 3). Weight loss and potentiostatic polarization measurements were used to investigate the inhibition efficiency of thiazole derivatives and the interaction mechanism between the inhibitors molecules and the copper surface. Effects of inhibitors concentration and temperature on the inhibitory behaviour of thiazoles were fully studied. The adsorption isotherm of inhibitors on copper surface and thermodynamic parameters were obtained and discussed in detail. Differences in inhibition performance of inhibitors were explained based on structural properties of investigated compounds.

2. EXPERIMENTAL

2.1. Materials

Tests were performed with copper of 99.99 wt.% purity. The molecular structures of the studied compounds, MFDT and TEBOT, are shown in Fig. 1.
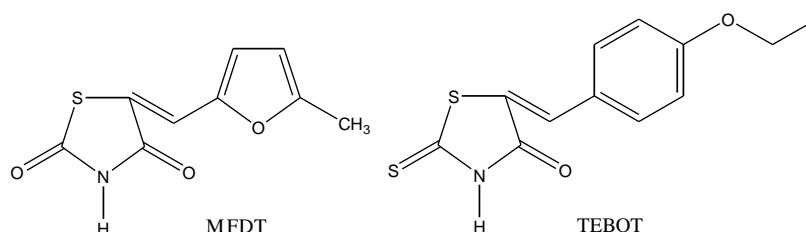

Figure 1. Molecular structures of two studied inhibitors.

These compounds are poorly soluble in water, but have good solubility in ethanol. Accordingly, the stock solution (5.0 x 10^{-4} mol dm^{-3}) was prepared by directly dissolving in ethanol, and then was diluted in 0.1 mol dm^{-3} Na_2SO_4 aqueous solutions containing 4% ethanol, by volume, for

solubility reasons. The concentration range of inhibitors was 1.0×10^{-6}–10.0×10^{-6} mol dm^{-3}. The pH values were adjusted to 3 by the addition of 10% H$_2$SO$_4$, prepared by dilution of 98% H$_2$SO$_4$ with distilled water. The solution in the absence of inhibitors was taken as blank for comparison. All test solutions were prepared from analytical grade chemical reagents without further purification. For each experiment, a freshly prepared solution was used.

2.2. Weight loss measurements

The copper rectangular specimens of 6.0 cm x 1.3 cm x 0.2 cm were abraded by a series of SiC paper (up to 1200 grit), washed with distilled water, and dried at room temperature. After weighing by digital balance (accuracy: ±0.1 mg), the specimens were immersed in 400 ml of 0.1 mol dm^{-3} Na$_2$SO$_4$ solutions (pH 3) without and with different concentrations of the inhibitors for 22 days at room temperature (25 ± 1 °C). All the investigated solutions were open to air. At the end of the tests, the specimens were taken out, washed with soft brush under running water to strip of the corrosion product, dried at room temperature, and weighed accurately again. Experiments were carried out in triplicate and the mean weight loss was reported. The maximum standard deviation in the observed weight loss was calculated to be ±5.0%.

2.3. Polarization measurements

Potentiostatic polarization measurements were conducted on a PGZ301 VoltaLab40 model potentiostat, controlled by a PC, supported by VoltaMaster4 software. Electrochemical experiments were carried out in the conventional three-electrode cell with a saturated calomel electrode (SCE) as the reference electrode, a platinum counter electrode and a copper working electrode. The copper electrode was in the form of disc, mounted into the epoxy resin to offer only one active flat surface exposed to the tested solution. The working surface area was 0.7 cm^2, and prepared as described above (Section 2.2). The working electrode was first immersed into the test solution for 1 h to establish a steady state open circuit potential (E_{ocp}). After measuring the E_{ocp}, polarization curves were obtained with a scan rate of 10 mV min^{-1} in the potential range between ±300 mV relative to the E_{ocp}. The tests were carried out at constant temperature of 15, 25, 35 and 45 °C (within ± 0.3 °C) by controlling the cell temperature using a water bath. All experiments were performed in atmospheric condition with stirring solutions.

3. RESULTS AND DISCUSSION

3.1. Effect of inhibitor concentration

3.1.1. Weight loss measurements

The inhibition effect of the investigated thiazole derivatives at different concentrations on the corrosion of copper in 0.1 mol dm^{-3} Na$_2$SO$_4$ solution (pH 3) was studied by weight loss measurements

at 25 °C after 22 days immersion. The corrosion rate (C_R) and percentage inhibition efficiency (η_w (%)) were calculated using the following equations:

$$C_R = \frac{W_o - W_i}{St} \tag{1}$$

$$\eta_w \, (\%) = \frac{C_{R(o)} - C_{R(i)}}{C_{R(o)}} \times 100 \tag{2}$$

where W_o and W_i are the average weight of specimen before and after immersion, respectively, S is the surface area of the specimen, t is the immersion time, $C_{R(o)}$ and $C_{R(i)}$ are the corrosion rates in the absence and presence of the inhibitor, respectively. Obtained results are given in Table 1. It can be noticed, that the C_R decreases and the η_w (%) increases with increasing concentration of each compound. This may be due to the increase of the adsorption and hence increasing the surface coverage of the inhibitors on the copper surface with increasing inhibitors concentration [18]. At the highest concentration (10.0×10^{-6} mol dm^{-3}) both thiazole derivatives exhibit maximum inhibition efficiency, and the inhibition performance follows the order of TEBOT > MFDT.

3.1.2. Potentiostatic polarization measurements

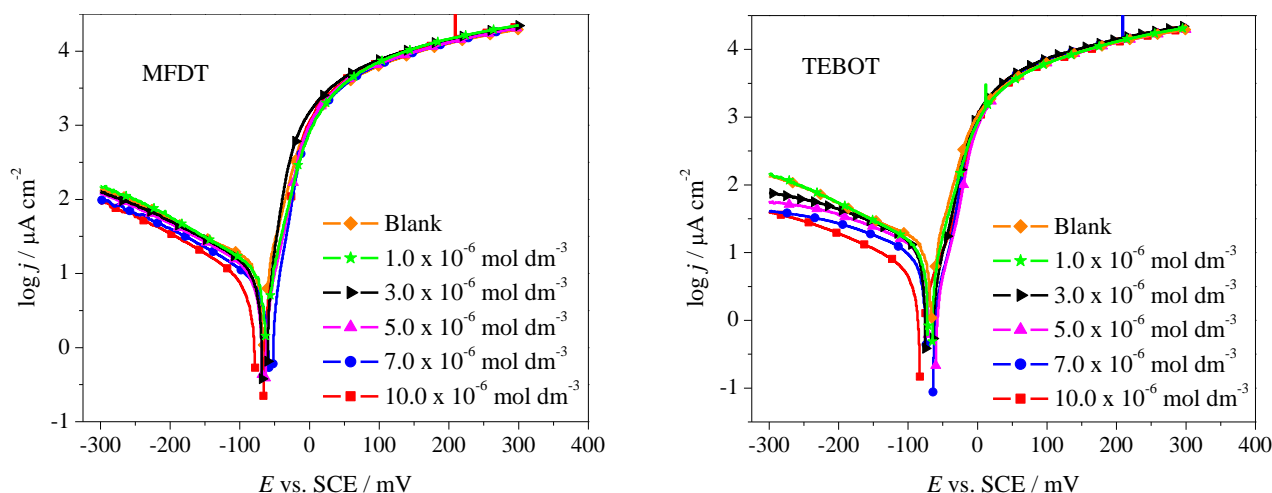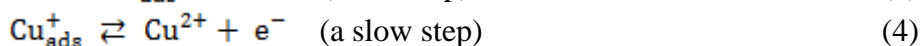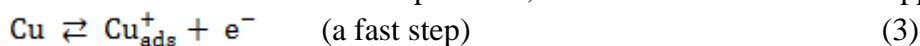**Figure 2.** Polarization curves for copper in 0.1 mol dm^{-3} Na$_2$SO$_4$ solution (pH 3) containing various concentrations of inhibitors at 25 °C.

In order to investigate the copper corrosion mechanism and effect of inhibitors concentration, potentiostatic polarization measurements were carried out in 0.1 mol dm^{-3} Na$_2$SO$_4$ solution (pH 3) in the absence and presence of different concentrations of MFDT and TEBOT. For the copper corrosion in aerated acidic solutions at corrosion potential, the anodic reaction is the copper dissolution:

$$\text{Cu} \rightleftarrows \text{Cu}^+_{ads} + e^- \qquad \text{(a fast step)} \tag{3}$$

$$\text{Cu}^+_{ads} \rightleftarrows \text{Cu}^{2+} + e^- \qquad \text{(a slow step)} \tag{4}$$

where Cu_{ads}^{+} is adsorbed at the copper surface and does not diffuse into the bulk solution. The reaction Eq. (4) is controlled by diffusion of soluble Cu^{2+} from the electrode surface to the bulk solution, which is generally the rate determining step [19]. The cathodic reaction is oxygen reduction:

$$O_2 + 4H^+ + 4e^- \rightleftarrows 2H_2O \tag{5}$$

Polarization curves for the copper electrode in 0.1 mol dm^{-3} Na$_2$SO$_4$ solution (pH 3) without and with different concentrations of MFDT and TEBOT at 25 °C are shown in Fig. 2.

As it can be seen from Fig. 2, after addition of investigated thiazole derivatives to 0.1 mol dm^{-3} Na$_2$SO$_4$ solution (pH 3) cathodic reaction was suppressed by the inhibitors to a greater extent than the anodic one. These results indicate that investigated compounds inhibit copper corrosion with predominant control of cathodic reaction.

The values of the corrosion current density (j_{corr}) and the corrosion potential (E_{corr}) obtained by Tafel extrapolation method, and percentage inhibition efficiency (η (%)) calculated by Eq. (6) are summarized in Table 1.

$$\eta\ (\%) = \frac{j_{corr\,(o)} - j_{corr\,(i)}}{j_{corr\,(o)}} \times 100 \tag{6}$$

where $j_{corr(o)}$ and $j_{corr(i)}$ represent the corrosion current density in the uninhibited and inhibited solution, respectively.

Table 1. Corrosion parameters obtained from chemical and electrochemical techniques, respectively, for copper in 0.1 mol dm^{-3} Na$_2$SO$_4$ solution (pH 3) containing various concentrations of inhibitors at 25 °C.

Inhibitor conc. (x 10^{-6} mol dm^{-3})	Weight loss measurements		Polarization measurements		
	C_R (mg cm^{-2} d^{-1})	η_w (%)	E_{corr} (mV)	j_{corr} (μA cm^{-2})	η (%)
Blank	0.25	-	-60	12.33	-
MFDT					
1.0	0.22	12.00	-58	11.32	8.19
3.0	0.20	20.00	-55	10.03	18.65
5.0	0.18	28.00	-51	8.94	27.49
7.0	0.16	36.00	-53	8.05	34.71
10.0	0.13	48.00	-59	6.44	47.77
TEBOT					
1.0	0.21	16.00	-57	10.62	13.87
3.0	0.18	28.00	-47	8.67	29.68
5.0	0.15	40.00	-39	7.31	40.71
7.0	0.12	52.00	-41	6.33	48.66
10.0	0.09	64.00	-54	4.63	62.45

Inspection of Table 1 revels that the j_{corr} values decrease in the presence of MFDT and TEBOT. The decreases of the corresponding current densities with increasing the inhibitors concentration were the consequence of the inhibitors adsorption on the copper surface [20]. It is also observed from results given in Table 1, that η (%) increases with increasing concentration of inhibitors, reaching the highest

value at a maximum concentration of 10.0 x 10^{-6} mol dm^{-3} for both of them. The order of efficiency according to polarization date is: TEBOT > MFDT. These results are in good agreement with those obtained from weight loss measurements. The distinction in the inhibition efficiency obtained by two techniques is mainly due to the fact that chemical technique provides average corrosion rate, while electrochemical technique gives instantaneous corrosion rate [21].

From Table 1 can find that the presence of inhibitors causes a minor change in E_{corr} values compared to the value for the blank solution. If the displacement in E_{corr} is more than 85 mV relating to the E_{corr} for the blank, the inhibitor can be classified as a cathodic or as anodic type [22]. The maximum displacement in our study is 18 mV and 21 mV, for MFDT and TEBOT, respectively, which suggest that inhibitors act as mixed type.

Good performance of thiazole derivatives as corrosion inhibitors for copper in 0.1 mol dm^{-3} Na$_2$SO$_4$ solution (pH 3) may be due to the presence of hetero-atoms, as well as those with conjugated double bonds or aromatic rings in their structures. To obtain better understanding of inhibition mechanism of MFDT and TEBOT, kinetic and thermodynamic studies were carried out.

3.2. Effect of temperature

The rise of temperature has an influence on the interaction between the copper electrode and the acidic solution in the absence and presence of inhibitors. Some of the polarization curves for copper in 0.1 mol dm^{-3} Na$_2$SO$_4$ solution (pH 3) with 1.0 x 10^{-6} mol dm^{-3} of MFDT and TEBOT in the temperature range 15–45 °C are given in Fig. 3.
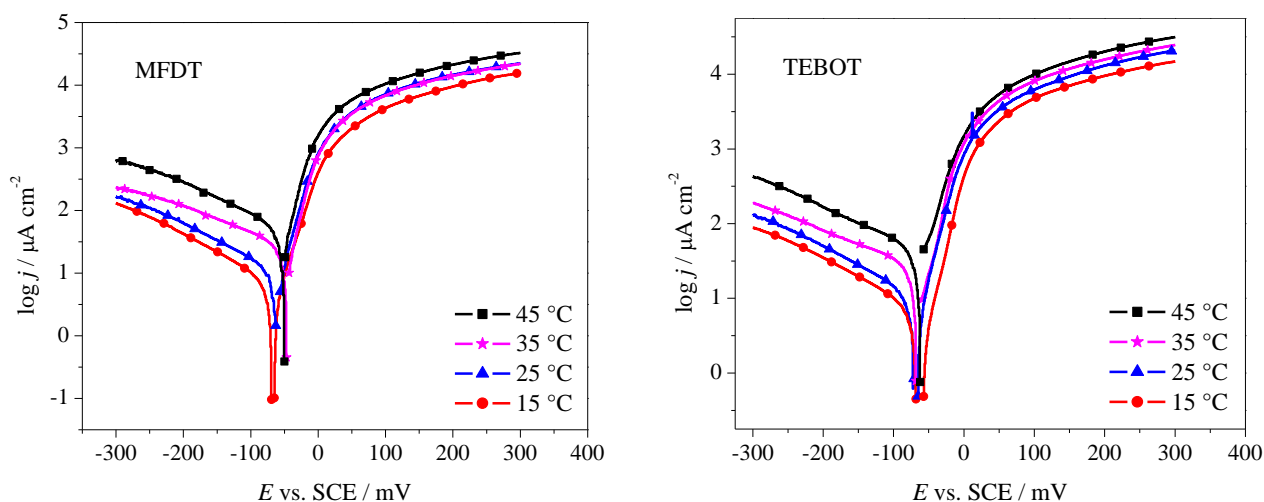

Figure 3. Effect of temperature on the polarization curves in 0.1 mol dm^{-3} Na$_2$SO$_4$ solution (pH 3) containing 1.0 x 10^{-6} mol dm^{-3} of inhibitors.

Table 2 and Table 3 show electrochemical parameters such as j_{corr} and E_{corr} calculated from Tafel plots. Values of η (%) and the degree of surface coverage (θ) for copper are also shown in these tables. The θ values were calculated from the following equation:

$$\theta = \frac{\eta\,(\%)}{100} \qquad\qquad\qquad\qquad (7)$$

As it can be seen from Table 2 and Table 3, the j_{corr} values increase with increasing temperature in the absence and presence of inhibitors, but this increase is more pronounced in the absence of inhibitors. These results suggest that MFDT and TEBOT act as efficient inhibitors in the studied temperature range. Table 2 and Table 3 also show that the η (%) values for MFDT and TEBOT increase with increasing temperature. Thus, the studied inhibitors efficiencies are temperature dependent. This increasing efficiency with increase in temperature can be described on the bases that adsorption and desorption of inhibitors molecules continuously occur at the metal surface and with increase of temperature the equilibrium between these two opposite process is shifted towards adsorption of the inhibitors molecules at the copper surface [23]. Such result also suggests that the adsorbed inhibitors are chemisorbed on the copper surface [24].

Table 2. Corrosion parameters obtained from polarization measurements for copper in 0.1 mol dm^{-3} Na$_2$SO$_4$ solution (pH 3) containing different concentrations of MFDT at various temperatures.

Temperature (°C)	Inhibitor conc. (x 10^{-6} mol dm^{-3})	E_{corr} (mV vs. SCE)	j_{corr} (μA cm^{-2})	η (%)	θ
15	Blank	-62	6.47	-	-
	1.0	-56	6.08	6.03	0.0603
	3.0	-52	5.50	14.99	0.1499
	5.0	-50	5.02	22.41	0.2241
	7.0	-43	4.57	29.37	0.2937
	10.0	-42	4.01	38.02	0.3802
25	Blank	-60	12.33	-	-
	1.0	-64	11.32	8.19	0.0819
	3.0	-55	10.03	18.65	0.1865
	5.0	-51	8.94	27.49	0.2749
	7.0	-50	8.04	34.71	0.3471
	10.0	-59	6.44	47.77	0.4777
35	Blank	-45	28.54	-	-
	1.0	-37	25.10	12.05	0.1205
	3.0	-36	20.81	27.08	0.2708
	5.0	-31	17.86	37.42	0.3742
	7.0	-30	15.46	45.83	0.4583
	10.0	-25	11.46	59.85	0.5985
45	Blank	-46	54.83	-	-
	1.0	-43	44.64	18.58	0.1858
	3.0	-41	33.97	38.04	0.3804
	5.0	-39	27.87	49.17	0.4917
	7.0	-44	22.82	58.38	0.5838
	10.0	-61	15.86	71.07	0.7107

The relationship between temperature and the rate of corrosion reaction is often expressed by the Arrhenius equation:

$$j_{corr} = A \exp\left(-\frac{E_a}{RT}\right) \tag{8}$$

where j_{corr} is the corrosion current density, that is directly proportional to the corrosion rate of copper in acidic media, A is the Arrhenius pre-exponential factor, E_a is the apparent activation energy, R is the universal gas constant, T is the absolute temperature. A plot of ln j_{corr} versus $1/T$ gives a straight line with a slope of $(-E_a/R)$ and an intercept of ln A. Arrhenius plots for the blank and different concentrations of TEBOT are given in Fig. 4. Similar plots for MFDT were obtained and not shown.

Table 3. Corrosion parameters obtained from polarization measurements for copper in 0.1 mol dm^{-3} Na$_2$SO$_4$ solution (pH 3) containing different concentrations of TEBOT at various temperatures.

| Temperature (°C)	Inhibitor conc. (x 10^{-6} mol dm^{-3})	E_{corr} (mV vs. SCE)	j_{corr} (µA cm^{-2})	η (%)	θ
15	Blank	-62	6.47	-	-
	1.0	-47	5.89	8.96	0.0896
	3.0	-39	5.04	22.10	0.2210
	5.0	-30	4.48	30.76	0.3076
	7.0	-32	3.98	38.49	0.3849
	10.0	-40	3.30	49.00	0.4900
25	Blank	-60	12.33	-	-
	1.0	-57	10.62	13.87	0.1387
	3.0	-47	8.67	29.68	0.2968
	5.0	-39	7.31	40.71	0.4071
	7.0	-41	6.33	48.66	0.4866
	10.0	-54	4.63	62.45	0.6245
35	Blank	-45	28.54	-	-
	1.0	-49	23.24	18.57	0.1857
	3.0	-48	17.56	38.47	0.3847
	5.0	-44	14.07	50.70	0.5070
	7.0	-44	11.73	58.90	0.5890
	10.0	-41	8.23	71.16	0.7116
45	Blank	-46	54.83	-	-
	1.0	-55	40.86	25.48	0.2548
	3.0	-45	27.87	49.17	0.4917
	5.0	-48	21.34	61.08	0.6108
	7.0	-46	17.05	68.90	0.6890
	10.0	-52	11.96	78.19	0.7819
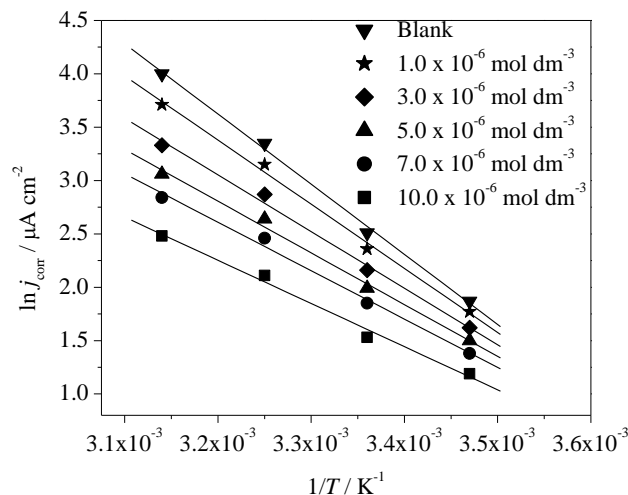
Figure 4. Arrhenius plots of ln j_{corr} vs. $1/T$ in the absence and presence of different concentrations of TEBOT.

Values of E_a and A for copper in 0.1 mol dm^{-3} Na$_2$SO$_4$ solution (pH 3) without and with various concentrations of MFDT and TEBOT are shown in Table 4.

Inspection of results in Table 4 shows that values of E_a obtained in the presence of both the inhibitors are lower than that obtained in the inhibitor free solution and decrease uniformly with the increase of inhibitors concentration. This reduction of the activation energy in the presence of thiazole derivatives is attributed to the chemisorption of the inhibitors molecules on the metal surface [25,26]. Table 4 also shows that the variance in A is similar to that in E_a. It is clear from Eq. (8) that the higher E_a and the lower A lead to lower j_{corr}. So in the present study, the decrease in j_{corr} is determined by the decrease of A.
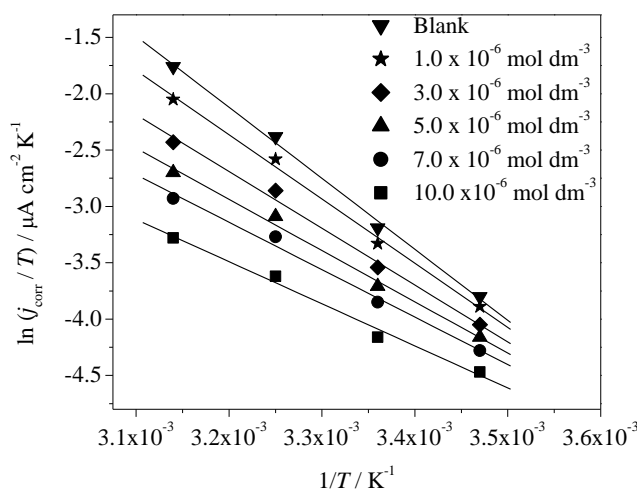

Figure 5. Transition state plots of ln (j_{corr}/T) vs. $1/T$ in the absence and presence of different concentrations of TEBOT.

The enthalpy of activation (ΔH_a^o) and the entropy of activation (ΔS_a^o) were obtained from the transition-state equation [27]:

$$j_{corr} = \frac{RT}{Nh} \exp\left(\frac{\Delta S_a^o}{R}\right) \exp\left(-\frac{\Delta H_a^o}{RT}\right) \tag{9}$$

where N is the Avogadro's number, h is the Planck's constant. A plot of ln (j_{corr}/T) against $1/T$ should give a straight line with a slope of $(-\Delta H_a^o/R)$ and an intercept of $[(\ln (R/Nh)) + (\Delta S_a^o/R)]$. Transition state plots for the blank and various concentrations of TEBOT are presented in Fig. 5. Analogous plots in the case of MFDT were obtained and not shown.

Obtained corrosion kinetic parameters for copper in 0.1 mol dm^{-3} Na$_2$SO$_4$ solution (pH 3) without and with various concentrations of MFDT and TEBOT are listed in Table 4.

As it can be seen from Table 4, the ΔH_a^o values are lower in the presence than in the absence of thiazole derivatives and decrease constantly with the increase of inhibitors concentration. The positive sign of ΔH_a^o values meaning the dissolution of copper is difficult in 0.1 mol dm^{-3} Na$_2$SO$_4$ solution (pH 3) [28]. Values of ΔS_a^o are large and negative without and with inhibitors and increase negatively with increasing inhibitors concentration. This implies that the activated complex in the rate determining step represents an association rather than a dissociation step, indicating that a decrease in disordering takes place on going from reactants to the activated complex [29].

Table 4. Corrosion kinetic parameters for copper in 0.1 mol dm^{-3} Na$_2$SO$_4$ solution (pH 3) in the absence and presence of different concentration of inhibitors.

Inhibitor conc. ($\times 10^{-6}$ mol dm^{-3})	E_a (kJ mol^{-1})	A (μA cm^{-2})	$\Delta H_a^{\ne}$ (kJ mol^{-1})	$\Delta S_a^{\ne}$ (J mol^{-1} K^{-1})
Blank	54.65	5.67 x 10^{10}	52.38	-47.56
MFDT				
1.0	51.09	1.22 x 10^{10}	48.83	-60.28
3.0	47.01	2.02 x 10^{9}	44.29	-76.68
5.0	44.22	5.72 x 10^{8}	41.72	-86.34
7.0	41.42	1.64 x 10^{8}	38.92	-96.68
10.0	35.45	1.17 x 10^{7}	32.88	-118.79
TEBOT				
1.0	49.96	7.25 x 10^{9}	47.39	-65.54
3.0	44.14	5.51 x 10^{8}	41.87	-85.92
5.0	40.29	9.70 x 10^{7}	37.79	-101.03
7.0	37.72	2.95 x 10^{7}	34.99	-111.67
10.0	33.63	4.25 x 10^{6}	31.06	-127.15

3.3. Adsorption isotherm and thermodynamic parameters

Values of θ obtained from polarization measurements, that corresponding to different concentrations of MFDT and TEBOT in the 15–45 °C temperature range (Table 2 and Table 3), were used to choose the best isotherm to determine the adsorption process. An efficient organic inhibitor

possesses the ability to be adsorbed at metal/solution interface by a substitution adsorption process as follow [30]:

$$Org_{(sol)} + XH_2O_{(ads)} \rightleftarrows Org_{(ads)} + XH_2O_{(sol)} \qquad (10)$$
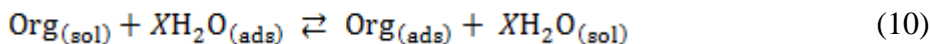
where $Org_{(sol)}$ and $Org_{(ads)}$ are the organic molecules in the solution and adsorbed on the metal surface, respectively, $H_2O_{(ads)}$ is the water molecules on the metal surface, X is the size ratio representing the number of water molecules substituted by one molecule of organic inhibitor. In order to determine the best fit between experimental results and isotherm functions, the mostly used adsorption isotherms such as Langmuir, Frumkin, Temkin and Bockris-Swinkels were tested. To choose isotherm that correlate with experimental date the best the correlation coefficient (R^2) was used. In the range of temperature studied (15–45 °C) the best description of the adsorption behavior of investigated thiazole derivatives was obtained using Bockris-Swinkels adsorption isotherm [31]:

$$K_{ads}C = \frac{\theta}{(1-\theta)^X} \frac{[\theta + X(1-\theta)]^{(X-1)}}{X^X} \qquad (11)$$

that is: $f(\theta) = K_{ads}C$, where K_{ads} is the equilibrium constant of the adsorption process, C is the inhibitor concentration. According to this isotherm a plot of the logarithm of the LHS of Eq. (11), $f(\theta)$, against logarithm of C should give a straight line with a slope of unity. For all the plots, straight lines were obtained with slopes close to 1.000 (Table 5) only when using a value of $X = 1$. This value means that one molecule of inhibitor adsorbed on metal surface replaces one water molecule. Fig. 6 shows such plots at different temperatures. All R^2 are up to 0.999 (listed in Table 5) indicating that Bockris-Swinkels adsorption isotherm fit well experimental date.
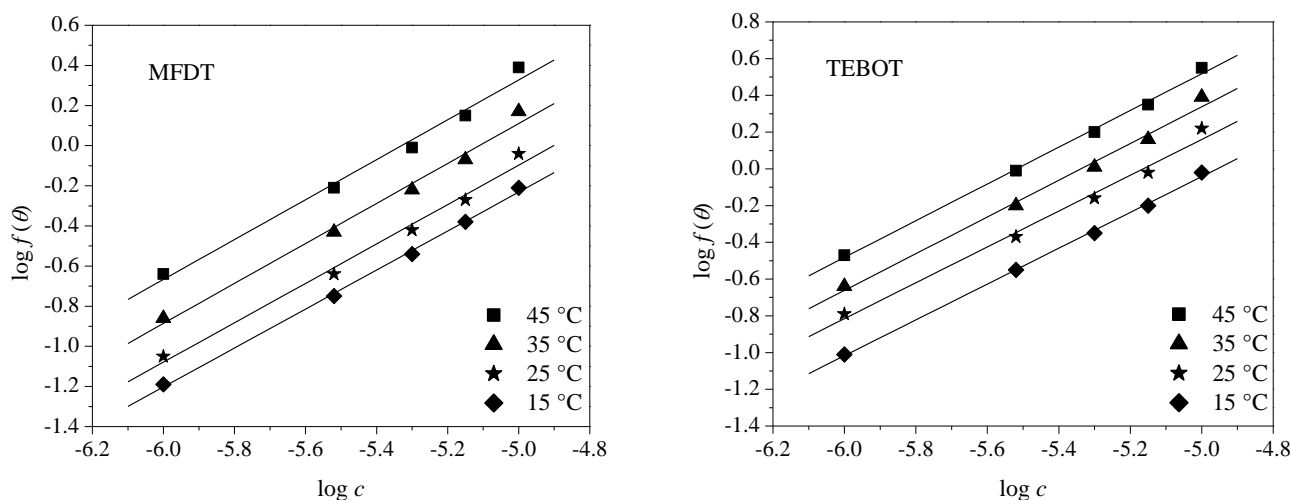

Figure 6. Bockris-Swinkels adsorption isotherm of inhibitors on copper surface in 0.1 mol dm^{-3} Na$_2$SO$_4$ solution (pH 3) at different temperatures.

From the intercepts of the straight lines the values of K_{ads} were calculated and given in Table 5. As can be seen, the K_{ads} values increase with the temperature for both the studied inhibitors, meaning that elevated temperature facilitates the adsorption of inhibitors. Generally, large value of K_{ads} implies strong adsorption of the inhibitor on the metal surface and hence better inhibition performance [32]. At a given temperature values of K_{ads} follow the order: TEBOT > MFDT, and so is with the efficiency.

Table 5. Thermodynamic parameters for the adsorption of inhibitors on the copper surface in 0.1 mol dm^{-3} Na$_2$SO$_4$ solution (pH 3) at different temperatures.

Temperature (°C)	Slope	R^2	K_{ads} (x 10^5 dm^3 mol^{-1})	ΔG°_{ads} (kJ mol^{-1})	ΔH°_{ads} (kJ mol^{-1})	ΔS°_{ads} (J mol^{-1} K^{-1})
MFDT						
15	0.971	0.999	0.42	-35.12	40.29	261.84
25	0.982	0.994	0.65	-37.41	40.29	260.74
35	0.996	0.995	1.24	-40.31	40.29	261.69
45	0.995	0.994	2.01	-42.90	40.29	261.60
TEBOT						
15	0.975	0.999	0.68	-36.28	40.97	268.23
25	0.976	0.994	1.10	-38.70	40.97	267.35
35	1.000	0.996	2.18	-41.76	40.97	268.60
45	1.000	0.998	3.31	-44.22	40.97	267.89

The K_{ads} is related to the standard free energy of adsorption (ΔG°_{ads}) according to:

$$K_{ads} = \frac{1}{55.5} \exp\left(\frac{-\Delta G^{\circ}_{ads}}{RT}\right) \tag{12}$$

where the value of 55.5 is the concentration of water in solution in mol dm^{-3}. The calculated values of ΔG°_{ads} are shown in Table 5.

Large negative values of ΔG°_{ads} are consistent with the spontaneity of the adsorption process and the stability of the adsorbed layer on the metal surface [33]. The ΔG°_{ads} values up to -20 kJ mol^{-1} or higher are related to the electrostatic interaction between the charged molecules and the charged metal surface (physisorption), while those more negative than -40 kJ mol^{-1} involve sharing or transfer of electrons from the inhibitor molecules to the metal surface to form a coordinate type of bond (chemisorption) [34]. In the present work, the values of ΔG°_{ads} are ranging between -35.12 and -42.90 kJ mol^{-1} for the adsorption of MFDT, and from -36.28 to -44.22 kJ mol^{-1} for the adsorption of TEBOT, indicating that the adsorption mechanism of investigated compounds on the copper at the studied temperatures is a mixed type involving two types of interactions physisorption and chemisorption. The adsorption of an organic molecule is not considered only as a physical or as chemical adsorption process [35]. However, temperature dependence of inhibition efficiency, as well as the reduction of the activation energy in the presence of additives suggest that adsorption of MFDT and TEBOT is mainly the chemisorption [36], accompanied by the physisorption. The ΔG°_{ads} values for both the thiazole derivatives increase negatively with temperature, further demonstrating that inhibitors at higher temperatures exhibit the stronger tendency to be adsorbed on copper surface. Absolute values of ΔG°_{ads} of the investigated compounds are in the order of TEBOT > MFDT. This is in good agreement with the range of the inhibition efficiency values obtained from both chemical and electrochemical techniques.

Thermodynamically, ΔG°_{ads} is related to the standard enthalpy and entropy of the adsorption process, ΔH°_{ads} and ΔS°_{ads}, respectively, through the thermodynamic basic equation:

$$\Delta G^{\circ}_{ads} = \Delta H^{\circ}_{ads} - T\Delta S^{\circ}_{ads} \tag{13}$$

The ΔH°_{ads} values were calculated using the Van't Hoff equation [37]:

$$\ln K_{ads} = -\frac{\Delta H^{\circ}_{ads}}{RT} + \text{constant} \tag{14}$$

Fig. 7 shows a plots of $\ln K_{ads}$ versus $1/T$ and slope of these straight lines is $(-\Delta H^{\circ}_{ads}/R)$.
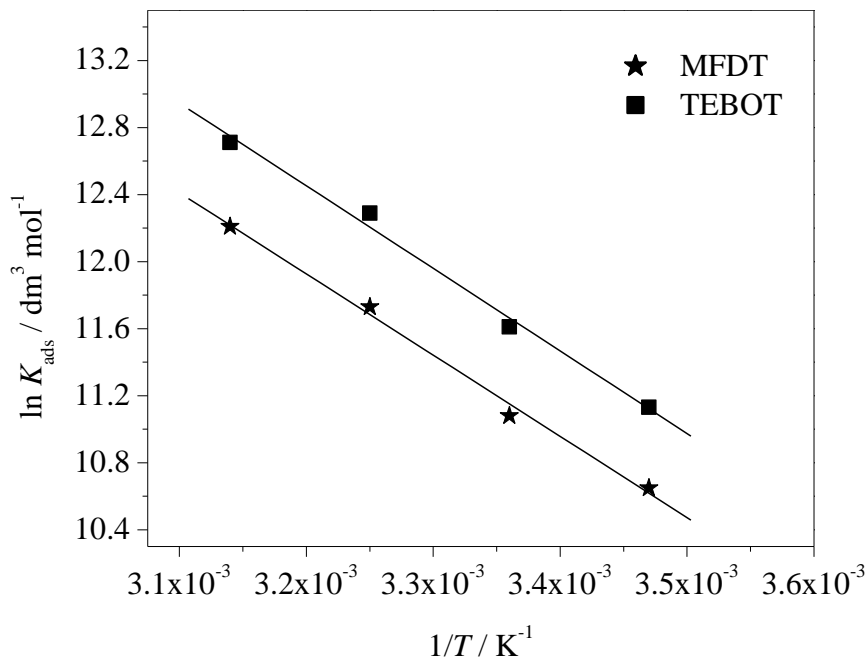

Figure 7. Van't Hoff plots for inhibitors adsorbed on copper surface in 0.1 mol dm^{-3} Na$_2$SO$_4$ solution (pH 3).

Then, values of ΔS°_{ads} were obtained by an alternative formulation of the Eq. (13):

$$\Delta S^{\circ}_{ads} = \frac{\Delta H^{0}_{ads} - \Delta G^{0}_{ads}}{T} \tag{15}$$

All obtained standard thermodynamic parameters are given in Table 5.

Positive values of ΔH°_{ads} indicate that the adsorption of inhibitors is an endothermic process. Endothermic adsorption process corresponds to chemisorption [38], which further confirms that adsorption of thiazole derivatives is complex in nature and predominantly chemisorption. Table 5 shows that the ΔS°_{ads} values are large and positive. The thermodynamic values obtained are the algebraic sum of the adsorption of organic molecules and desorption of water molecules, since in this situation the adsorption of organic inhibitor is accompanied by desorption of water molecules [39]. Therefore, the positive values of ΔS°_{ads} are attributed to the increase in the solvent entropy and to more positive water desorption entropy [40]. The positive sign of the ΔS°_{ads} values also means that an increase in disordering takes place on going from reactants to the metal-adsorbed species reaction complex [41,42], which is the driving force for the adsorption of inhibitor on copper surface [42].

Values of ΔH°_{ads} and ΔS°_{ads} are also calculated from Eq. (13). A plot of ΔG°_{ads} versus T gives straight lines as shown in Fig. 8.
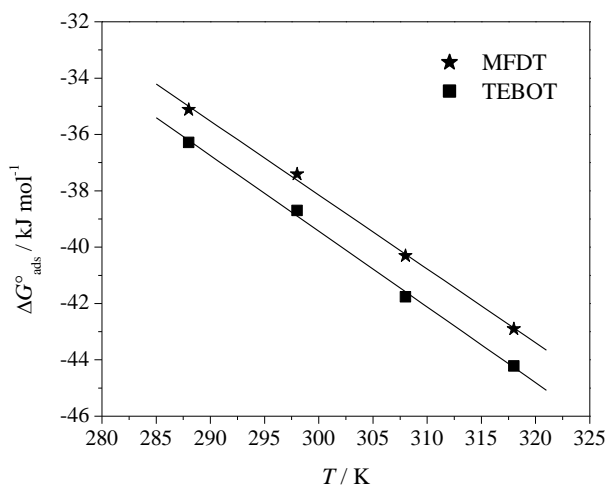
Figure 8. Variation of $\Delta G^{\mathrm{o}}_{\mathrm{ads}}$ with T for copper in 0.1 mol dm^{-3} Na$_2$SO$_4$ solution (pH 3) containing inhibitors.

The slope of the straight lines is $-\Delta S^{\mathrm{o}}_{\mathrm{ads}}$, and the intercept is $\Delta H^{\mathrm{o}}_{\mathrm{ads}}$. Calculated $\Delta H^{\mathrm{o}}_{\mathrm{ads}}$ values of 40.57 and 41.21 kJ mol^{-1} for MFDT and TEBOT, respectively, are very close to that obtained using the Van't Hoff equation. Moreover, the deduced $\Delta S^{\mathrm{o}}_{\mathrm{ads}}$ values of 262.40 and 268.80 J mol^{-1} K^{-1} for MFDT and TEBOT, respectively, are very close to that obtained in Table 5. Values of thermodynamic parameters obtained by two methods are in good agreement.

3.4. Adsorption mechanism and inhibitor structure

The mechanism of the inhibition process of the corrosion inhibitors under consideration is mainly the adsorption one. The process of adsorption is influenced by the nature and charge surface of the metal, the type of aggressive electrolyte, the chemical structure of the inhibitor and the distribution of charge over the whole inhibitor molecule [43].

The adsorption of tested compounds can be attributed to the presence of hetero atoms (O, N and S), carbonyl, >C=S, -CH=C< group and aromatic rings (furan and benzene). Therefore, the possible reaction centres are unshared electron pairs of hetero atoms and π-electrons of carbonyl, >C=S, -CH=C< group and aromatic rings (furan and benzene).

Generally, owing to the complex nature of adsorption and inhibition of a given inhibitors, it is impossible for single adsorption mode between inhibitors and metal surface. The adsorption and inhibition effect of MFDT and TEBOT in 0.1 mol dm^{-3} Na$_2$SO$_4$ solution (pH 3) can be explained as follows. Both thiazole derivatives might be protonated in the acidic solution as:

$$\mathrm{MFDT} + x\mathrm{H}^+ \rightleftarrows [\mathrm{MFDTH}_x]^{x+} \tag{16}$$

$$\mathrm{TEBOT} + x\mathrm{H}^+ \rightleftarrows [\mathrm{TEBOTH}_x]^{x+} \tag{17}$$
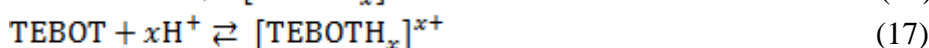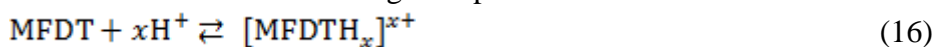
Thus, in aqueous acidic solutions, investigated compounds exist either as neutral molecules or cations.

In general, two modes of adsorption could be considered. According to results of temperature dependence of inhibition efficiency, and obtained kinetic (E_a) and thermodynamic parameters (ΔG^o_{ads}, ΔH^o_{ads}), the neutral MFDT and TEBOT molecules may be adsorbed on the copper surface through the chemisorption mechanism, involving the displacement of water molecules from the metal surface and the sharing electrons between the hetero atoms and copper. The inhibitor molecules can be also adsorbed on the copper surface on the bases of donor-acceptor interactions between π-electrons and vacant d-orbitals of metal. On the other hand, the values of ΔG^o_{ads} indicate the contribution of physical adsorption. It is thought that the copper surface bears positive charge in acidic environment [44]. Thus, because of the electrostatic repulsion, it is difficult for the protonated $[MFDTH_x]^{x+}$ and $[TEBOTH_x]^{x+}$ to approach the positively charged metal surface. The protonated organic inhibitors can be adsorbed on the copper surface via SO_4^{2-} ions, which form the interconnecting bridges between the positively charged metal surface and the protonated molecules [45].

As already mentioned earlier, the inhibition efficiency of examined thiazole derivatives follow the order: TEBOT > MFDT. The performance of the studied inhibitors depends on the electron donating properties of the substituent, -CH$_3$ and -OC$_2$H$_5$ in the MFDT and TEBOT, respectively. The presence of electron donating groups, -CH$_3$ and -OC$_2$H$_5$, increases the electron density of furan ring in the MFDT and benzene ring in the TEBOT, respectively, and leading to easier electron transfer from the functional groups (furan and benzene) to the metal, resulting in high inhibition efficiency. Ethoxy group is better electron donor than methyl group, hence TEBOT shows better performance as corrosion inhibitor in comparison with MFDT. Apart from that, TEBOT exhibits better efficiency than MFDT because of the deeper interaction caused by the presence of one more S atom, instead of O atom detected in the MFDT, since η (%) increases in the order O < S. Moreover, better performance of TEBOT can be attributed to its higher molecular weight (265 g mol^{-1}) compared with MFDT (209 g mol^{-1}), so TEBOT covers larger area of copper than MFDT.

4. CONCLUSIONS

1.   Both investigated thiazole derivatives, MFDT and TEBOT, inhibit the corrosion of copper in 0.1 mol dm^{-3} Na$_2$SO$_4$ solution (pH 3). Inhibition efficiency increases with increasing the concentration of inhibitors and follows the order: TEBOT > MFDT.

2.   The inhibition behavior obtained from weight loss measurements show the same trend as noticed in the potentiostatic polarization measurements.

3.   Based on the values of E_{corr} obtained from polarization curves both MFDT and TEBOT behave as mixed type inhibitors, but marked decrease in the cathodic current density in the presence of inhibitors suggests that this compounds act as predominantly cathodic type inhibitors in 0.1 mol dm^{-3} Na$_2$SO$_4$ solution (pH 3).

4.   Inhibition efficiency also increases with temperature, which leads to decrease of activation corrosion energy.

5. The adsorption of either MFDT or TEBOT obeys Bockris-Swinkels adsorption isotherm ($X = 1$). The adsorption process is an endothermic process accompanied by an increase in entropy.

6. The trend of inhibition efficiency with temperature and the parameters of apparent activation energy, standard free energy of adsorption and standard enthalpy of the adsorption process indicate that the adsorption is mainly the chemisorption.

7. The better inhibition efficiency of TEBOT than MFDT could be explained inhibitors structure.

References

1. D. Gelman, D. Starosvetsky, Y. Ein-Eli, *Corros. Sci.*, 82 (2014) 271.
2. M. Behpour, N. Mohammadi, *Corros. Sci.*, 65 (2012) 331.
3. W. Chen, S. Hong, H.B. Li, H.Q. Luo, M. Li, N.B. Li, *Corros. Sci.*, 61 (2012) 53.
4. K.S. Lokesh, M. De Keersmaecker, A. Elia, D. Depla, P. Dubruel, P. Vandenabeele, S. Van Vlierberghe, A. Adriaens, *Corros. Sci.*, 62 (2012) 73.
5. J. Fu, J. Pan, Z. Liu, S. Li, Y. Wang, *Int. J. Electrochem. Sci.*, 6 (2011) 2072.
6. X. He, Y. Jiang, C. Li, W. Wang, B. Hou, L. Wu, *Corros. Sci.*, 83 (2014) 124.
7. J. Aljourani, K. Raeissi, M.A. Golozar, *Corros. Sci.*, 51 (2009) 1836.
8. H. Tian, W. Li, K. Cao, B. Hou, *Corros. Sci.*, 73 (2013) 281.
9. M. Behpour, S.M. Ghoreishi, N. Soltani, M. Salavati-Niasari, *Corros. Sci.*, 51 (2009) 1073.
10. S.E. Nataraja, T.V. Venkatesha, K. Manjunatha, B. Poojary, M.K. Pavithra, H.C. Tandon, *Corros. Sci.*, 53 (2011) 2651.
11. M.M. Antonijevic, M.B. Petrovic, *Int. J. Electrochem. Sci.*, 3 (2008) 1.
12. S.J. Kashyap, V.K. Garg, P.K. Sharma, N. Kumar, R. Dudhe, J.K. Gupta, *Med. Chem. Res.*, 21 (2012) 2123.
13. A.V. Shanbhag, T.V. Venkatesha, R.A. Prabhu, B.M. Praveen, *Bull. Mater. Sci.*, 34 (2011) 571.
14. M.L. Zheludkevich, K.A. Yasakau, S.K. Poznyak, M.G.S. Ferreira, *Corros. Sci.*, 47 (2005) 3368.
15. M.A. Quraishi, H.K. Sharma, *J. Appl. Electrochem.*, 35 (2005) 33.
16. K.F. Khaled, M.A. Amin, *Corros. Sci.*, 51 (2009) 1964.
17. Gy. Vastag, E. Szocs, A. Shaban, I. Bertoti, K. Popov-Pergal, E. Kalman, *Solid State Ionics*, 141–142 (2001) 87.
18. D. Wang, B. Xiang, Y. Liang, S. Song, C. Liu, *Corros. Sci.*, 85 (2014) 77.
19. R. Solmaz, E. A. Sahin, A. Donerb, G. Kardas, *Corros. Sci.*, 53 (2011) 3231.
20. I. Ahamad, R. Prasad, M.A. Quraishi, *Corros. Sci.*, 52 (2010) 3033.
21. Z. Tao, W. He, S. Wang, S. Zhang, G. Zhou, *Corros. Sci.*, 60 (2012) 205.
22. E.S. Ferreira, C. Giacomelli, F.C. Giacomelli, A. Spinelli, *Mater. Chem. Phys.*, 83 (2004) 129.
23. M. Yadav, S. Kumar, D. Behera, I. Bahadur, D. Ramjugernath, *Int. J. Electrochem. Sci.*, 9 (2014) 5235.
24. I.O. Arukalam, *Carbohyd. Polym.*, 112 (2014) 291.
25. M. Behpour, S.M. Ghoreishi, N. Soltani, M. Salavati-Niasari, M. Hamadanian, A. Gandomi, *Corros. Sci.*, 50 (2008) 2172.

26. X. Wang, Y. Wan, Y. Gu, Y. Ma, F. Shi, W. Nui, Q. Wang, *Int. J. Electrochem. Sci.*, 9 (2014) 1840.
27. J.O'M. Bockris, A.K.N. Reddy, *Modern Electrochemistry*, Plenum Press, New York, (1977).
28. A.K. Singh, M.A. Quraishi, *Corros. Sci.*, 52 (2010) 152.
29. D. Ben Hmamou, R. Salghi, A. Zarrouk, H. Zarrok, B. Hammouti, S.S. Al-Deyab, A. El Assyry, N. Benchat, M. Bouachrine, *Int. J. Electrochem. Sci.*, 8 (2013) 11526.
30. A. Zarrouk, I. Warad, B. Hammouti, A. Dafali, S.S. Al-Deyab, N. Benchat, *Int. J. Electrochem. Sci.*, 5 (2010) 1516.
31. J.O'M. Bockris, D.A.J. Swinkels, *J. Electrochem. Soc.*, 111 (1964) 736.
32. X. Li, X. Xie, S. Deng, G. Du, *Corros. Sci.*, 87 (2014) 27.
33. M.A. Ameer, A.M. Fekry, A. Othman, *Int. J. Electrochem. Sci.*, 9 (2014) 1964.
34. M. Bozorg, T.S. Farahani, J. Neshati, Z. Chaghazardi, G.M. Ziarani, *Ind. Eng. Chem. Res.*, 53 (2014) 4295.
35. R. Yıldız, A. Doner, T. Dogan, I. Dehri, *Corros. Sci.*, 82 (2014) 125.
36. M. Mobin, S. Masroor, *Int. J. Electrochem. Sci.*, 7 (2012) 6920.
37. D.D. Do, *Adsorption Analysis: Equilibria and Kinetics*, Imperial College Press, New York, (1998).
38. D. Daoud, T. Douadi, S. Issaadi, S. Chafaa, *Corros. Sci.*, 79 (2014) 50.
39. I. Ahamad, R. Prasad, M.A. Quraishi, *Corros. Sci.*, 52 (2010) 1472.
40. B. Ateya, B. El-Anadauli, F.El Nizamy, *Corros. Sci.*, 24 (1984) 509.
41. F. Bentiss, M. Lebrini, M. Lagrenee, *Corros. Sci.*, 47 (2005) 2915.
42. S. Deng, X. Li, X. Xie, *Corros. Sci.*, 80 (2014) 276.
43. A.O. Yuce, G. Kardas, *Corros. Sci.*, 58 (2012) 86.
44. K.F. Khaled, *Corros. Sci.*, 52 (2010) 3225.
45. K. Mallaiyaa, R. Subramaniama, S.S. Srikandana, S. Gowria, N. Rajasekaranb, A. Selvarajc, *Electrochim. Acta*, 56 (2011) 3857.